In vitro reconstitution of Bluetongue virus infectious cores

Sofia Lourenco and Polly Roy[1]

Department of Pathogen Molecular Biology, Faculty of Infectious and Tropical Diseases, London School of Hygiene and Tropical Medicine, London WC1E 7HT, United Kingdom

Edited* by Aaron J. Shatkin, Center for Advanced Biotechnology and Medicine, Piscataway, NJ, and approved July 13, 2011 (received for review May 31, 2011)

Bluetongue virus (BTV) is a vector-borne, nonenveloped icosahedral particle that is organized in two capsids, an outer capsid of two proteins, VP2 and VP5, and an inner capsid (or core) composed of two major proteins, VP7 and VP3, in two layers. The VP3 layer (subcore) encloses viral transcription complex (VP1 polymerase, VP4 capping enzyme, VP6 helicase) and a 10-segmented double-stranded (dsRNA) genome. Although much is known about the BTV capsids, the order of the core assembly and the mechanism of genome packaging remain unclear. Here, we established a cell-free system to reconstitute subcore and core structures with the proteins and ssRNAs, demonstrating that reconstituted cores are infectious in insect cells. Furthermore, we showed that the BTV ssRNAs are essential to drive the assembly reaction and that there is a distinct order of internal protein recruitment during the assembly process. The in vitro engineering of infectious BTV cores is unique for any member of the *Reoviridae* and will facilitate future studies of RNA-protein interactions during BTV core assembly.

assembly pathway | Orbivirus | engineered particle

Bluetongue virus (BTV) is a member of family *Reoviridae* and the prototype of the Orbivirus genus. BTV and other orbiviruses are vectored to vertebrates by arthropod species and replicate in both hosts. The BTV particles are nonenveloped, architecturally complex particles organized in two capsids. The icosahedral inner capsid, or core, with a diameter of 75 nm, is composed of two protein layers, the surface layer of 260 trimers of VP7 (38 kDa) that is built on a thin scaffold made up of 60 dimers of VP3 (100 kDa) (1–3). The VP3 layer, although serving as the scaffold for deposition of VP7 molecules, also encloses a viral genome of 10 double-stranded RNA (dsRNA) segments of discrete sizes, together with the viral transcription complex of three proteins, VP1 (RNA-dependent RNA polymerase), VP4 (capping enzyme), and VP6 (RNA helicase) (reviewed in ref. 4) and is termed the "subcore" (5). The outer capsid is composed of VP2 and VP5, which are necessary for virus entry in mammalian cells (2, 5, 6). In infected cells BTV encodes four additional nonstructural proteins (NS1, NS2, NS3, and NS3A), which are involved in virus replication and morphogenesis (7–10). BTV virions enter into the mammalian cells via an endocytic pathway where the particle is uncoated (removal of VP2 and VP5) to release core particles into the cytosol (5, 11). This release triggers core transcription activities, where the enclosed 10 ssRNA transcripts are synthesized repeatedly and extruded continuously via pores located at the 12 vertices of the icosahedral core. These transcripts serve as templates for synthesis of progeny genomic dsRNA segments and also as mRNAs that direct protein synthesis (3, 5). Transcriptionally active cores can be derived in vitro from purified virions by proteolytic treatment and are capable of infecting insect *Culicoides* cells (12).

In virus-infected cells, the viral inclusion bodies (VIBs), which are predominantly driven by viral-encoded NS2, act as the assembly sites for core components (7, 13). Interestingly, in the absence of genomic RNA or NS2 (VIBs), core-like particles (CLPs) of VP3 and VP7 are assembled via the baculovirus expression system, essentially mimicking the size and molar ratio of each protein in the native cores (14). Furthermore, the CLPs could also successfully recruit VP1 and VP4 but not VP6 (15). This system has been used extensively to understand the protein–protein interactions involved in VP3 and VP7 assembly and to some extent between the VP3, VP1, and VP4 proteins (16–18). However, the assembly of complete cores has not been possible using this system. Thus, because of lack of an appropriate assay system for BTV and other members of the *Reoviridae* family, several outstanding questions in the replication cycle still remain to be addressed: (*i*) the sequence of events leading to the assembly of a BTV core, (*ii*) the importance of ssRNAs in this process, and (*iii*) the sorting and packaging of the 10 ssRNA segments.

In this study we have established a cell-free system to reconstitute BTV subcores and core particles and demonstrated that the reconstituted particles are not only competent for generation of genomic dsRNAs from ssRNA templates, but are infectious in *Culicoides* cells (KC cells), synthesizing both viral proteins and genomic 10 dsRNAs. Furthermore, this unique system has allowed us to define the essential steps required for subcore and core assembly and, in part, to determine the order of the assembly process. Our data demonstrated that recruitment of ssRNAs is essential to drive the functional core assembly.

This in vitro reconstitution system will be useful to address further questions for better understanding of the BTV assembly pathway and RNA packaging mechanisms, as well as having potential for extrapolating to other dsRNA viruses.

Results

In Vitro Reconstitution of BTV Subcore. Previous studies using the baculovirus expression system failed to generate fully assembled BTV cores and, thus, it has not been possible to investigate the essential steps in the assembly pathway. Therefore, we decided to establish an alternative cell-free–based assembly system for examining BTV intermediates of subcores and core formation. Before this process, it was necessary to ensure that each core protein (VP1, VP4, VP6, VP3, and VP7) could be synthesized in vitro. As shown in Fig. S1, all five core proteins, from 38 KD (VP7) to 150 KD (VP1) were synthesized and could be detected by Western blot using specific polyclonal antibodies for each protein. The system was then used for the generation of BTV subcores.

We hypothesized that the transcription complex (TC) proteins and positive sense ssRNA should be assembled before VP3 assembly. Thus, the optimized assembly assay consisted of a pretranslation of each of the TC proteins individually (VP1, VP4, VP6), followed by the addition of 10 in vitro synthesized T7-derived uncapped transcripts (as described in ref. 19). The TC complex and 10 ssRNAs were allowed to interact for 60 min, then

Author contributions: S.L. and P.R. designed research; S.L. performed research; S.L. and P.R. analyzed data; and S.L. and P.R. wrote the paper.

The authors declare no conflict of interest.

*This Direct Submission article had a prearranged editor.

[1]To whom correspondence should be addressed. E-mail: Polly.Roy@lshtm.ac.uk.

This article contains supporting information online at www.pnas.org/lookup/suppl/doi:10.1073/pnas.1108667108/-/DCSupplemental.

VP3 was added to the mixture, and incubation was continued for further 90 min. The reaction mixture was fractionated on a continuous 15% to 65% sucrose gradient and 10 fractions (from the top of the gradient) were collected and analyzed both by native- and SDS-PAGE, followed by silver staining and Western blot.

The silver-stained native gel showed that only fraction 6 consisted of high molecular-mass bands (significantly heavier than 669 kDa) (Fig. 1*A*). Furthermore, the Western analysis of the SDS-PAGE showed that all four subcore proteins (Fig. 1*B*) were present in the same fractions. Control wheat germ extracts lacking any BTV protein or ssRNA were similarly analyzed but showed no bands on a native gel (Fig. 1*C*).

To verify if the assembled complex had also recruited the 10 ssRNA molecules, ssRNAs were ^{32}P-labeled and a similar assembly assay was undertaken and processed as described. Fraction 6 was analyzed for the presence of ssRNAs by denaturing agarose gel. Fig. 2 shows the typical profile of the 10 segments of BTV ssRNAs, indicating a successful recruitment of ssRNA into, or associated with, the putative subcore complex.

Recruitment of BTV ssRNAs Is Essential for Assembly of the Subcore Structures. Because the above studies indicated that 10 ssRNAs were recruited or associated with the high molecular-weight complexes that were consistent with a subcore-like complex, we varied the assay to investigate their role in the assembly process. An assembly assay was performed as above but followed by RNase One treatment to specifically degrade ssRNAs before sucrose gradient fractionation. The fractions were analyzed directly on a 1% denaturing agarose gel to detect ssRNAs. No RNA was detected in any of the fractions (Fig. 3*A*, *Left*), in contrast to the untreated sample (Fig. 3*A*, *Right*, fractions 5 and 6), where they were present, albeit less discrete than seen in Fig. 2 because of the presence of sucrose, which changed the RNA migration. Thus, recruited ssRNAs were not protected from RNase activity. Native gel analysis of the same samples showed that the complex formed in fractions 5 and 6 in the absence of RNase One (Fig. 3*B*, *Right*) was no longer detectable after RNase treatment (Fig. 3*B*, *Left*). This finding was further confirmed by the absence of detectable proteins by Western blot in the expected fractions (5 and 6, observed from the untreated equivalent, Fig. 3*C*, *Right*). These results indicate that the ssRNAs were not protected by the putative assembled subcore and that the presence of RNA appeared to be essential for this assembly process.

Reconstitution of BTV Cores in Vitro. As the template 10 ssRNAs were not protected from RNase degradation by the assembled subcore-like complex, it seemed likely that pores described in the VP3 layer (20) of the core structure might allow RNase access.

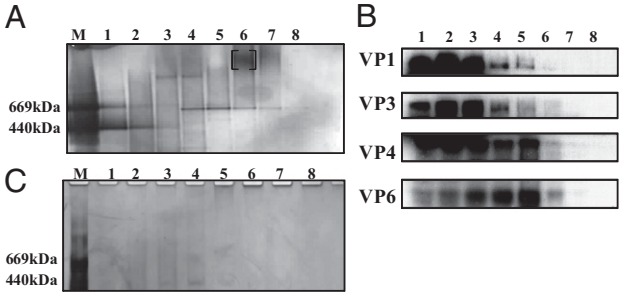

Fig. 1. Assembly of a complex with subcore components. After the assembly assay, the reaction mixture was purified on a continuous sucrose gradient; the fractions (1–8) were analyzed on native gel followed by silver staining (*A*) and on 10% SDS-PAGE followed by Western blots (*B*). The complex formation is indicated. (*C*) Wheat germ extracts lacking any BTV protein or RNA were tested similarly and analyzed on native gel followed by silver staining.

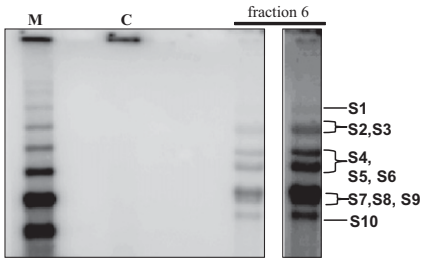

Fig. 2. Recruitment of ssRNAs by the putative subcore complex. The sucrose fraction containing the complex (fraction 6) was phenol/chlorophorm-extracted, precipitated, and resuspended in denaturing formaldehyde loading buffer and analyzed by 1% agarose denaturing gel. The ssRNAs of the fraction 6 and the position of each segment are indicated. (*Right*) The longer exposure of the same. C: fraction 9 processed similarly as negative control. M: ^{32}P-labeled marker ssRNAs (Promega).

Assembly of the VP7 layer onto the VP3 layer plugs these pores, which only opens up when the core becomes transcriptionally active in the presence of nucleoside triphosphates (rNTPs) (21). Therefore, we hypothesized that the addition of VP7 to the putative subcores might protect the incorporated 10 ssRNAs.

We attempted the in vitro reconstitution of cores by addition of VP7 to the assembly assay. The assay conditions remained unmodified except for the sequential addition of VP7, and after the incubation the reaction was either treated or not with RNase One and fractionated as before. In contrast to the above data, ssRNAs were present in the treated sample, although at slightly lighter fractions (fractions 4 and 5) than the untreated equivalent (fractions 5 and 6) (Fig. 4*A*). To ensure the activity of the RNase One, a commercially available ssRNA marker was added to wheat germ extract in 45% sucrose and incubated similarly (Fig. 4*A*, *Center*). We confirmed the activity of the RNase One, which degraded the ssRNA marker (Fig. 4*A*, lane +, *Center*), and also confirmed that when the sucrose fractions were analyzed without phenol-

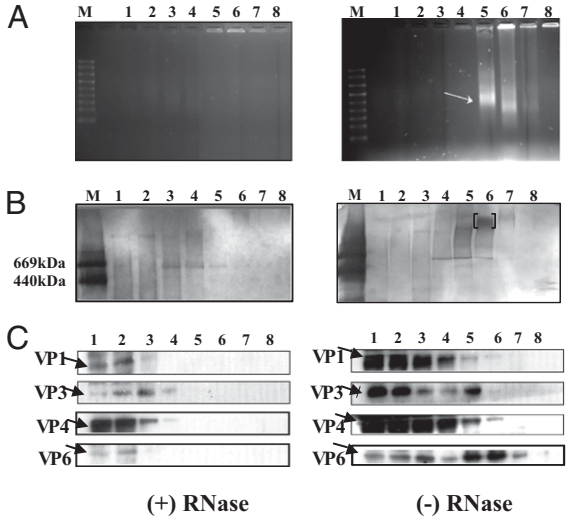

Fig. 3. RNase sensitivity of ssRNAs in the subcore complex. (*A*) The subcore assembly reaction was directly loaded onto the sucrose gradient or treated with 0.125 U/μL Rnase One (Promega) at 37 °C for 30 min before fractionation. The fractions (1–8) were analyzed by 1% denaturing agarose gel followed by ethidium bromide staining. Although the RNase One untreated sample (*Right*) shows the presence of ssRNAs (arrow), the treated sample (*Left*) has no RNA. (*B*) Samples were also analyzed by native gels followed by silver staining. The RNA-protein complex (putative subcores) is indicated. (*C*) Western blots of the same samples. Arrows show the position of each protein.

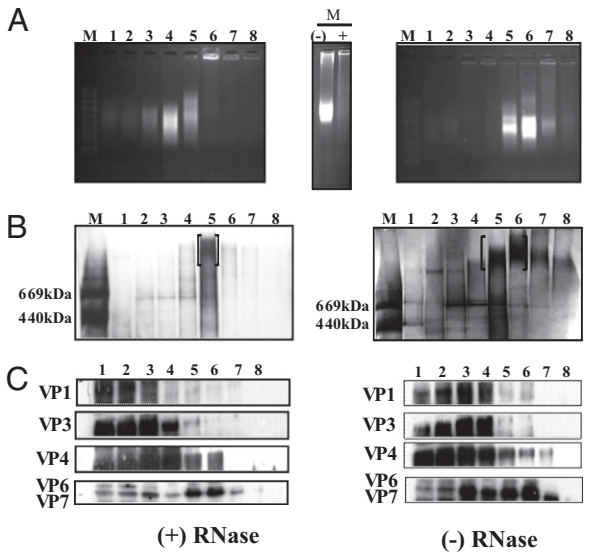

Fig. 4. Putative cores protect ssRNAs from RNase treatment. (*A*) The core assembly reaction was directly (*Right*) loaded onto the sucrose gradient or treated (*Left*) with 0.125 U/μL Rnase One (Promega) at 37 °C for 30 min before fractionation and fractions were analyzed by 1% denaturing agarose gel followed by ethidium bromide staining. A control reaction of RNA marker mixed with wheat germ extracts and 45% sucrose was processed similarly (*Center*). (*B*) Samples were also analyzed by native gels and silver-stained. Putative cores are indicated. (*C*) Western blots of the same samples.

chloroform extraction, the ssRNA no longer had a discrete pattern [Fig. 4*A*, lane (–), *Center*, comparing to M lane, *Right* and *Left*].

Because ssRNAs were protected upon VP7 addition, the complex formed could be a putative core. High molecular-weight material was detected in the native gels (Fig. 4*B*) for both treated and untreated samples (Fig. 4*B*) and the presence of all core proteins was confirmed by Western blots (Fig. 4*C*). Note that high amounts of all proteins were observed in the lighter fractions (e.g., fractions 1–4) than fraction 6, indicating that not all proteins were assembled. Interestingly, after RNase treatment, the complex was shifted to a lighter fraction, both in the native gel (the position of cores is indicated in Fig. 4*B*) and in the Western blots (Fig. 4*C*), similar to that observed for the ssRNAs gel (Fig. 4*A*). This finding might be a result of excess and free RNAs attached to cores but degraded upon the addition of RNase. Therefore, after RNase treatment the complex would be lighter than the untreated equivalent. Supporting this observation, the VP3 levels in the putative cores were lower than expected. When quantification of Fig. 4*C* (*Right*, for fraction 6) was performed by ImageJ and band intensity normalized to VP1 (band 1), the in vitro-assembled core profile had the following ratio: 1:1.5:3.5:4.1:80 for VP1:VP3:VP4:VP6:VP7, respectively. From previous studies, the native core profile is expected as 1:10:3:5:70 (4, 14–16, 20). Thus, putative cores are low in VP3 and likely represent a mixture of part assembled and complete particles. Furthermore, the enhanced levels of VP7 might be a result of some aggregation. Nevertheless, within those cores assembled on a complete VP3 layer, the ssRNAs were protected and the assembly was not impaired by the RNase treatment. These observations confirmed that ssRNAs recruited within the subcores were not protected because of the absence of VP7.

The presence of the 10 ssRNAs in this system appeared to be essential for the assembly of subcores, providing the initial architecture for core formation maintaining all components together.

Reconstituted Cores Possess Enzyme Activity. It has been hypothesized that newly synthesized 10 ssRNA transcripts are first recruited with assembling subcore proteins before acting as templates for genomic dsRNA synthesis in infected cells (reviewed in ref. 2). We wanted to determine if the packaged ssRNAs in the reconstituted cores could act as templates for synthesis of genomic dsRNA segments. Thus, after the addition of VP3 to the assembly assay, rNTPs together with ^{32}P-CTP were added to the reaction mixture to trigger VP1-mediated replicase activity before the addition of VP7. After completion of the reaction, nonrecruited RNAs were removed by RNase A digestion (degrades both dsRNA and ssRNA). The putative synthesized dsRNAs were extracted from fractions 5 and 6, precipitated, and analyzed on a 9% native-PAGE. The viral genomic dsRNAs were prepared from native BTV1 cores and used as markers. The dsRNAs of the in vitro putative cores were resistant to RNase A and exhibited similar profiles to that of the native dsRNAs (Fig. 5*A*). These data demonstrated that the reconstituted cores were functional and the packaged ssRNAs could indeed act as templates for dsRNA synthesis inside the core structure.

BTV VP1 is capable of dsRNA synthesis in vitro in the absence of the other proteins and dsRNA could also bind BTV cores surface (22, 23). It was therefore necessary to eliminate the possibility of dsRNAs generated by unpackaged VP1, binding and packaging of dsRNAs within the cores. Thus, the assembly assay was performed in presence of ^{32}P-labeled dsRNAs instead of ssRNAs and gradient fractions were analyzed before and after RNase A treatment. As shown in Fig. 5*B*, dsRNA in fractions 5 and 6 could clearly be detected before RNase A treatment, but not after treatment. Thus, the dsRNAs detected on fractions 5 and 6 in this assay were not packaged but bound to the core surface. Furthermore, it confirmed that the dsRNAs detected in Fig. 5*A* were indeed generated because of the activity of the VP1 on recruited ssRNA templates within the reconstituted putative cores.

Because the in vitro reconstituted putative BTV cores were replication competent, we investigated if these assembled particles were morphologically similar to native cores. Fraction 6 was therefore visualized by electron microscopy (EM). Several

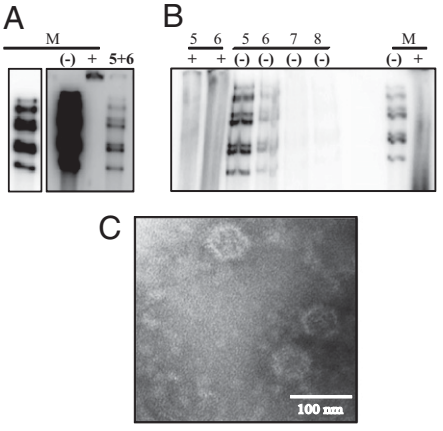

Fig. 5. Polymerase activity of putative cores and dsRNA packaging assay. (*A*) Synthesis of dsRNAs from the packaged ssRNAs templates in the transcription complex was undertaken in the presence of rNTPs and ^{32}P labeled CTP, as described in *Materials and Methods*. The products of the polymerase assay were treated with RNase A (Sigma), fractionated, phenol-chlorophorm extracted, and analyzed on 9% native PAGE (lanes 5 and 6). As a positive control, purified dsRNAs of BTV1 (lane M) were ^{32}P-labeled at the 3′ ends, analyzed similarly, or treated with RNase A before analysis; (*Left*) the untreated marker at a lower exposure. (*B*) The same assembly assay was performed in presence of ^{32}P-labeled dsRNAs, gradient-fractionated, and either directly analyzed on a 9% PAGE, or after RNase A treatment. Lanes 5 and 6: RNase A treated (+); lanes 5 to 8: fractions 5 to 8, untreated (–); M: Purified ^{32}P-labeled dsRNAs of BTV1, treated (+) or untreated (–) with RNase A. (*C*) Sample from fraction 6 was processed by EM. (Scale bar, 100 nm.)

particulate structures resembling native cores could be detected by negative staining under EM (Fig. 5*C*).

In Vitro Reconstituted Cores Are Infectious. Native cores lacking the two outer capsid proteins are capable of establishing infection in insect vector cells (12). We took advantage of this fact to investigate whether reconstituted cores had functional components and were capable of establishing a productive infection. Post-reconstituted fractions were used directly to infect insect cells (KC cells) and viral protein expressions were monitored by immunofluorescence assay. Three different proteins were tested: two nonstructural proteins, NS1 and NS2 that are abundantly expressed in virus-infected cells, and VP5, an outer capsid protein. These proteins were not present in the assembly assay. All tested proteins were detected when an aliquot of fraction 6 was used for infection (Fig. 6 *A* and *B*). Furthermore, their distributions were similar to the natural infection: NS1, highly expressed, located in the cytoplasm (Fig. 6*A*, in green); NS2 showed the typical punctuate patterns (Fig. 6*B*, in green); and VP5 exhibited a homogenous pattern at the edges of the cells (Fig. 6*B*, in red). None of the proteins were detected in cells infected with fraction 4 or in the uninfected cells (Fig. 6 *C* and *D*).

The putative progeny viruses grown in KC cells from fractions 5, 6, and 7 were further passaged four times and genomic dsRNA segments were isolated. The purified dsRNAs of fraction 6-infected cells showed typical patterns of authentic BTV1 dsRNAs (Fig. 6*E*), confirming that the reconstituted cores were appropriately assembled, morphologically and genetically correct, and were infectious. Some dsRNA bands were also observed in fraction 5 (lane 2), most likely because of incomplete formation of cores and defective replication. No dsRNA was detected in fraction 7 or in uninfected KC cells.

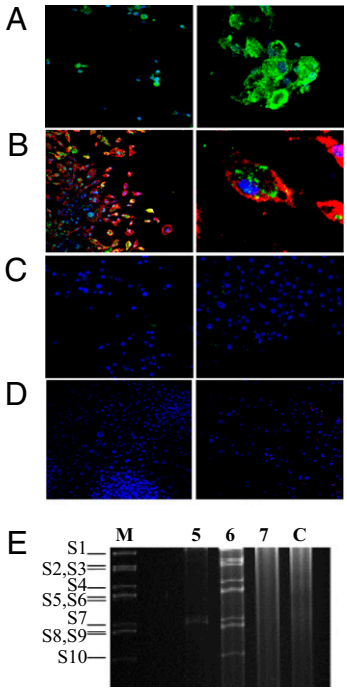

Fig. 6. In vitro-generated cores are infectious in insect cells. Core assembly reaction mix was processed as above; KC cells were infected with each fraction and expression of BTV proteins were examined by immunofluorescence assay. (*A*) NS1 staining (green) of fraction 6-infected KC cells (Magnification: 20×). (*Right*) Higher amplification (Magnification: 40×). (*B*) NS2 (green) and VP5 (red) staining of the same (Magnification: 20×). (*Right*) Higher amplification (Magnification: 40×). (*C*) Representative of uninfected (*Left*) and fraction 4-infected KC cells (*Right*) stained with anti-NS1 (Magnification: 20×). (*D*) Representative of uninfected (*Left*) and fraction 4-infected KC cells (*Right*) stained with both anti-NS2 and anti-VP5 (Magnification: 20×). (*E*) Putative virus was passaged in KC cells four times and dsRNAs were extracted and analyzed on a 9% native-PAGE followed by ethidium bromide staining. Lanes, 5, 6, 7: dsRNAs extracted from KC cells infected with fractions 5, 6, and 7, respectively; lane M: dsRNAs extracted from BTV1 infected cells; lane C: uninfected KC cells processed similarly, as a negative control.

Interaction Between Different Combinations of the Replication Complex Proteins. The in vitro system established appeared to mimic the viral core assembly pathway. Therefore, we further exploited it to determine the order of events that occur during the subcore assembly. We tested different combinations of subcore proteins (two, three, or four proteins) in the presence of the 10 uncapped ssRNAs. After the assembly assays and fractionation on sucrose gradient, as described above, each gradient fraction was analyzed by native gels (Fig. S2 shows the relevant fractions for each combination). For each combination tested, a protein-RNA complex was detected in only one of the fractions. That band corresponding to each complex was quantified and normalized to the native protein marker to generate a quantitative graph (Fig. 7). Fig. 7 demonstrates that the most efficient assembly was achieved when all four proteins were present, as expected. When combinations of three proteins were compared, the assembly efficiency of VP1+VP3+VP6, where VP4 was lacking, was less efficient than the other three combinations (VP1+VP4+VP6, VP1+VP3+VP4, VP3+VP4+VP6). This observation implies that VP4 plays a central role for the complex formation. When only two proteins were used, the most efficient complex was VP1+VP4, significantly better than the VP3+VP4, VP4+VP6, or VP1+VP6 combinations. However, VP1+VP3 or VP3+VP6 were the least efficient, suggesting that VP1 interacts predominantly with VP4 and VP6 and the best interacting partner for VP3 was VP4.

Taken together, these results suggest that VP1 interacts first with VP4 and VP6 before the interaction with VP3, most likely via VP4, to stabilize the complex. It is noteworthy that all these combinations were tested in the presence of the 10 ssRNAs. In agreement with the previous data shown in this study, ssRNAs are likely to drive the assembly of intermediates that include VP6.

Assembly was also tested in the absence of the entire set of 10 uncapped ssRNAs and in the presence of only nine segments (S10 was excluded). Fig. S3 shows that assembly can still occur in the absence of added ssRNAs, although we cannot exclude the role of

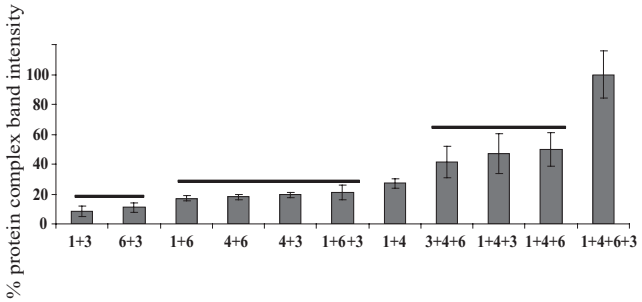

Fig. 7. Assembly of subcore intermediates. The different protein combinations were used for assembly (either two or three), fractionated and the fractions were analyzed by native gels, followed by silver staining (see Fig. S2 for an example of the relevant fractions). The bands corresponding to a protein complex were quantified by ImageJ software, normalized to the bands of the native high molecular-weight marker (GE Healthcare), and calculated in percentages for the intensity of the bands. As a positive control, assembly of all four subcore proteins was similarly analyzed and was set as 100% of assembly efficiency. The graph of these values is shown. The SD was calculated from three independent experiments. Each group marked by a bar is significantly different from each other, $P < 0.05$ by Student *t* test.

MICROBIOLOGY

residual untranslated RNA (used as templates for protein translation) in the formation of the complex. When S10 was excluded, we observed complex assembly but the failure to incorporate the nine remaining segments suggesting a key role for S10 in the recruitment of genome segments. The precise functional basis for this mechanism remains to be examined.

Discussion

In this article we have developed an in vitro assay to assess the assembly processes of BTV. Our previous attempts using a baculovirus expression system were unsuccessful in encapsidation of VP1, VP4, and VP6 simultaneously into baculovirus-expressed CLPs (composed of VP3 and VP7) or virus-like particles (composed of VP2, VP3, VP5, and VP7) (14, 24). Nevertheless, these studies have provided us with valuable information in relation to the assembly pathway and protein–protein interacting domains of these four major proteins. Their structures and functions, including their immunogenic properties, were important for rationally designed vaccines (25).

The unique in vitro cell-free assembly assay system presented in this article allowed us to reconstitute subcores (VP1, VP4, VP6, and VP3) and cores (VP1, VP4, VP6, VP3, and VP7) with the complete set of 10 viral ssRNA molecules.

The role of ssRNAs in BTV subcore and core assembly has so far not been studied because of the lack of an appropriate system. The unique system established in this study allowed us to show the recruitment of 10 ssRNA exact copies into the subcores and cores. The RNase One digestion (which degrades ssRNA) of the in vitro assembled subcores clearly demonstrated that these structures did not provide protection to the packaged RNAs. This finding is not surprising as the VP3 layer possesses distinct pores. Furthermore, after RNase treatment, RNA degradation led to the disassembly of the subcore particulate structure, indicating that ssRNA recruitment is essential for its assembly to occur. These observations set BTV apart from bacteriophages φ6 and φ8 of *Cystoviridae* family, in which the assembly takes place in the absence of RNA and its reconstitution was possible, expressing in vitro each viral protein in *Escherichia coli*. The RNA is then packaged a posteriori to the formation of procapsids (26–28).

The addition of VP7 provided complete protection to the packaged ssRNAs from RNase One digestion. Interestingly, the RNase One-treated sample appeared in a lighter fraction than the untreated equivalent. This finding could be a result of the degradation of ssRNA/dsRNA associated with the outside of the core (23). The resulting putative cores were therefore lighter, free of unpackaged RNA, which could interact nonspecifically with intermediate protein complexes and nascent cores.

VP7 is thus essential to protect the recruited ssRNAs and maintain all components together, as required for core formation. A low level of VP3 detected in the Western blots for the fraction containing putative cores is consistent with the presence of a mixed population. However, the other four proteins were present in similar ratios to native cores.

To confirm the activity of the generated in vitro cores, we performed a polymerase assay. We clearly demonstrated that dsRNAs were synthesized from the reconstituted putative cores. The possibility of dsRNAs generated by free VP1 interacting on the outside of the cores and being packaged was also eliminated. This study is unique in having such RNA-protein complexes entirely reconstituted in vitro, and more importantly, in showing that the recruited ssRNAs were used as templates for the generation of genomic dsRNAs being the putative core enzymatically active. These results fit the hypothesis in which the ssRNAs are recruited before the formation of a mature core and are used as templates for dsRNA synthesis during the assembly pathway, leading to the generation of complete cores.

Additionally, the putative cores appeared morphologically and dimensionally similar to native cores under EM. These properties encouraged us to undertake an infectivity test of the engineered cores. A productive infection was successfully obtained in KC cells, supported by: (*i*) the expression of proteins that were absent from the input assembly assay, (*ii*) the distribution pattern of these proteins in the cell, and (*iii*) the recovery of dsRNA with the expected profile after the passage of the putative core in KC cells. The uniqueness of the system developed in this report presents key advantages: (*i*) it is rapid, not requiring the time-consuming expression and purification of each protein; (*ii*) it mimics, to a certain extent, native conditions; (*iii*) it allows the study of RNA-protein and protein–protein interactions; (*iv*) it can target one specific step under study, which is not possible in a cell-based system; and (*v*) productive infection could be achieved from the reconstituted putative cores.

This facile system further allowed us to generate some information on the sequence of events and intermolecular interactions occurring during the assembly pathway. We were able to demonstrate that VP4 interacts with each of the subcore proteins. In addition, VP6 interacts with VP4 and VP1, previously hypothesized but not shown until now. Cryo-EM studies have shown that VP1 and VP4 are closely located inside the core structure and lie directly under VP3 layer (16). This study is unique in demonstratingVP4/VP6 interactions, as well as the incorporation of VP1/VP4/VP6 TC in subcores. This result could be because of the presence of the 10 ssRNAs in our system, allowing RNA-protein interactions, which seemed essential for the assembly to occur and appeared important for VP6 packaging.

Despite the uniqueness of the system and its use for understanding various steps of core assembly, it has certain limitations. For example, it is a small scale technique and some nonspecific interactions cannot be avoided; in addition, some intermediate complexes are also generated, the structure of which could be interesting to define, as these may be necessary to lead to a mature core.

In summary, this system allowed us to: (*i*) uniquely clarify the sequence of events occurring during the assembly pathway by testing different combinations of subcore proteins; (*ii*) demonstrate clearly that the 10 ssRNAs were required for the subcore assembly, uniquely obtaining an in vitro packaging of all core components; and (*iii*) uniquely generate entirely in vitro assembled cores, which were enzymatically active, morphologically similar to native cores under EM and infectious in KC cells.

We provided therefore a unique system that can be used for RNA-protein interactions, mapping of packaging signals, and to some extent, structural studies. The packaging process is so far poorly understood, although preliminary data shown here suggest that the assembly of proteins continues in the absence of one of the 10 segments, but that the packaging of the remaining nine segments is impaired. This topic is currently under study and will be the focus of future studies.

In the future, it would be interesting to characterize more deeply the biochemical and structural properties of the obtained subcores and putative cores, as well as their intermediates. This system could be applied to other dsRNA viruses, such as other members of the *Reoviridae* family.

Materials and Methods

In Vitro Translation of VP1, VP3, VP4, VP6, and VP7. For in vitro translation of capped ssRNAs, wheat germ extracts (Promega) were used according to the manufacturer's instructions. DNA constructs are described in *SI Materials and Methods* and primers are listed in Table S1. Protein synthesis was identified by Western blot.

Assembly Assay. To reconstitute subcores, VP1, VP4, and VP6 in vitro translations were carried out individually for 30 min at 25 °C, then mixed together in presence of 10 BTV1 ssRNAs followed by further incubation for 60 min at 25 °C. VP3 in vitro translation reaction was added later to the mix, to allow its translation in the presence of the other three proteins and the ssRNAs, followed by incubation for 90 min at 25 °C. For the generation of putative cores, VP7 was added sequentially after the addition of VP3 and incubated for

90 min at 25 °C. The reaction mixture was loaded on a 15% to 65% continuous sucrose gradient for 90 min at 200,000 × *g* at 4 °C, using a TLS55 rotor. Fractions were collected from the top and the putative complex formation was determined by detecting the presence of BTV proteins on a native gels followed by silver staining, as well as on a 10% SDS-PAGE followed by Western blot. Presence of the 10 ssRNAs was analyzed by electrophoresis on a 1% agarose gel in Mops (morpholinepropanesulfonic acid) buffer in the presence of formaldehyde, followed by ethidium bromide staining. The procedure was performed in a category 2 laboratory in an isolated and virus-free room dedicated to RNA work.

Polymerase Assay. The assembly assay was performed as described above. After the addition of VP3 translation mix to the assembly assay and incubation for 90 min at 25 °C, 160 μM rATP, rGTP, rUTP, 1 μM rCTP, 0.4 μCi/μL α^{32}P CTP (Amersham Biosciences) were incorporated to the mix. The wheat germ extracts already contain Mg^{2+} in a final concentration of 2 mM. After an incubation of 90 min at 25 °C, VP7 was added and incubated a further 90 min. The reaction was treated with RNase A for 30 min at 37 °C to degrade both ssRNAs and any residual dsRNAs outside the cores. The mix was then loaded on a continuous 15% to 65% sucrose gradient and processed as above. Samples were analyzed by 9% native-PAGE, dried, and exposed to a Storage Phosphor screen (GE Healthcare).

ACKNOWLEDGMENTS. We thank Maria McCrossan for technical help with the electron microscopy experiments and Ian Jones for critical review of the manuscript and helpful comments. This work is supported jointly by the Biotechnology and Biological Sciences Research Council (United Kingdom) and the National Institute of Health (United States).

1. Fukusho A, Yu Y, Yamaguchi S, Roy P (1989) Completion of the sequence of bluetongue virus serotype 10 by the characterization of a structural protein, VP6, and a non-structural protein, NS2. *J Gen Virol* 70:1677–1689.
2. Roy P (2008) Functional mapping of bluetongue virus proteins and their interactions with host proteins during virus replication. *Cell Biochem Biophys* 50(3):143–157.
3. Verwoerd DW, Huismans H (1972) Studies on the in vitro and the in vivo transcription of the bluetongue virus genome. *Onderstepoort J Vet Res* 39(4):185–191.
4. Roy P (2008) Bluetongue virus: Dissection of the polymerase complex. *J Gen Virol* 89: 1789–1804.
5. Verwoerd DW, Els HJ, De Villiers EM, Huismans H (1972) Structure of the bluetongue virus capsid. *J Virol* 10:783–794.
6. Forzan M, Marsh M, Roy P (2007) Bluetongue virus entry into cells. *J Virol* 81: 4819–4827.
7. Kar AK, Bhattacharya B, Roy P (2007) Bluetongue virus RNA binding protein NS2 is a modulator of viral replication and assembly. *BMC Mol Biol* 8:4.
8. Hyatt AD, Zhao Y, Roy P (1993) Release of bluetongue virus-like particles from insect cells is mediated by BTV nonstructural protein NS3/NS3A. *Virology* 193:592–603.
9. Celma CC, Roy P (2009) A viral nonstructural protein regulates bluetongue virus trafficking and release. *J Virol* 83:6806–6816.
10. Celma CC, Roy P (2011) Interaction of calpactin light chain (S100A10/p11) and a viral NS protein is essential for intracellular trafficking of nonenveloped bluetongue virus. *J Virol* 85:4783–4791.
11. Huismans H, van Dijk AA, Els HJ (1987) Uncoating of parental bluetongue virus to core and subcore particles in infected L cells. *Virology* 157(1):180–188.
12. Mertens PP, Burroughs JN, Anderson J (1987) Purification and properties of virus particles, infectious subviral particles, and cores of bluetongue virus serotypes 1 and 4. *Virology* 157:375–386.
13. Modrof J, Lymperopoulos K, Roy P (2005) Phosphorylation of bluetongue virus nonstructural protein 2 is essential for formation of viral inclusion bodies. *J Virol* 79: 10023–10031.
14. French TJ, Roy P (1990) Synthesis of bluetongue virus (BTV) corelike particles by a recombinant baculovirus expressing the two major structural core proteins of BTV. *J Virol* 64:1530–1536.
15. Loudon PT, Roy P (1991) Assembly of five bluetongue virus proteins expressed by recombinant baculoviruses: Inclusion of the largest protein VP1 in the core and virus-like proteins. *Virology* 180:798–802.
16. Nason EL, et al. (2004) Interactions between the inner and outer capsids of bluetongue virus. *J Virol* 78:8059–8067.
17. Kar AK, Ghosh M, Roy P (2004) Mapping the assembly pathway of Bluetongue virus scaffolding protein VP3. *Virology* 324:387–399.
18. Limn CK, Staeuber N, Monastyrskaya K, Gouet P, Roy P (2000) Functional dissection of the major structural protein of bluetongue virus: Identification of key residues within VP7 essential for capsid assembly. *J Virol* 74:8658–8669.
19. Boyce M, Celma CC, Roy P (2008) Development of reverse genetics systems for bluetongue virus: Recovery of infectious virus from synthetic RNA transcripts. *J Virol* 82: 8339–8348.
20. Grimes JM, et al. (1998) The atomic structure of the bluetongue virus core. *Nature* 395:470–478.
21. Diprose JM, et al. (2001) Translocation portals for the substrates and products of a viral transcription complex: The bluetongue virus core. *EMBO J* 20:7229–7239.
22. Boyce M, Wehrfritz J, Noad R, Roy P (2004) Purified recombinant bluetongue virus VP1 exhibits RNA replicase activity. *J Virol* 78:3994–4002.
23. Diprose JM, et al. (2002) The core of bluetongue virus binds double-stranded RNA. *J Virol* 76:9533–9536.
24. French TJ, Marshall JJ, Roy P (1990) Assembly of double-shelled, viruslike particles of bluetongue virus by the simultaneous expression of four structural proteins. *J Virol* 64:5695–5700.
25. Roy P, French T, Erasmus BJ (1992) Protective efficacy of virus-like particles for bluetongue disease. *Vaccine* 10(1):28–32.
26. Poranen MM, Paatero AO, Tuma R, Bamford DH (2001) Self-assembly of a viral molecular machine from purified protein and RNA constituents. *Mol Cell* 7:845–854.
27. Kainov DE, Butcher SJ, Bamford DH, Tuma R (2003) Conserved intermediates on the assembly pathway of double-stranded RNA bacteriophages. *J Mol Biol* 328:791–804.
28. Kainov DE, et al. (2003) RNA packaging device of double-stranded RNA bacteriophages, possibly as simple as hexamer of P4 protein. *J Biol Chem* 278:48084–48091.